Mapping the Cu-BTC metal-organic framework (HKUST-1) stability envelope in the presence of water vapour for CO_2 adsorption from flue gases

Nadeen Al-Janabi,[a] Patrick Hill,[a] Laura Torrente-Murciano,[b] Arthur Garforth,[a] Patricia Gorgojo,[a] Flor Siperstein,[a] Xiaolei Fan*, [a]

[a] *School of Chemical Engineering and Analytical Science, The University of Manchester, Oxford Road, Manchester, UK*
[b] *Department of Chemical Engineering, University of Bath, Bath, UK*

ABSTRACT

Cu-BTC Metal-organic framework (HKUST-1) was evaluated as the model material for CO_2 capture from flue gas streams. This paper presents an optimised hydrothermal synthesis of HKUST-1 and an analysis of water stability of HKUST-1. Substantial improvements of the hydrothermal synthesis process of HKUST-1 are shown to increase the quantitative yield up to 89.4% at 100ºC. Single-component adsorption experiments were carried out under conditions relevant for flue gases adsorption (45–60ºC, 0–1 barG) to evaluate the performance of HKUST-1 in terms of adsorption capacity, showing that the amount adsorbed of water can reach up to 21.7 mmol g^{-1}, about one order of magnitude higher than CO_2 (1.75 mmol g^{-1}) and almost two orders of magnitude higher than N_2 (0.17 mmol g^{-1}). The hydration process of HKUST-1 framework was investigated using dynamic vapour adsorption under the flue gas emitting conditions. HKUST-1 is sensitive to humid streams and dynamic deformation of its porous structure takes place at 40–50ºC and various relative humidity values, leading to the irreversible decomposition of HKUST-1 framework and the consequent deterioration in its adsorption capacity. Under humid conditions, water displaces the organic linkers from the copper centres causing the collapse of HKUST-1 framework. These results provide fundamental knowledge to enable future material design for the modification of the hydrophilic nature of copper sites in HKUST-1 to improve its moisture stability.

Keywords: Metal-organic frameworks (MOFs); HKUST-1; hydrothermal synthesis, flue gas; water vapour adsorption; stability.

HIGHLIGHTS:

- Improved hydrothermal synthesis of HKUST-1 at 100ºC with the yield up to 89.4%.
- Evaluation moisture stability of HKUST-1 under relevant flue gas adsorption conditions (45–60ºC, 0–1 barG).
- Interpretation of decomposition dynamics of HKUST-1 under humid conditions.
- Aggregation of water molecules near copper centres can displace the BTC ligands leading to the decomposition of HKUST-1.

GRAPHICAL ABSTRACT

* Corresponding author. Tel.: +44 1613062690; email address: xiaolei.fan@manchester.ac.uk

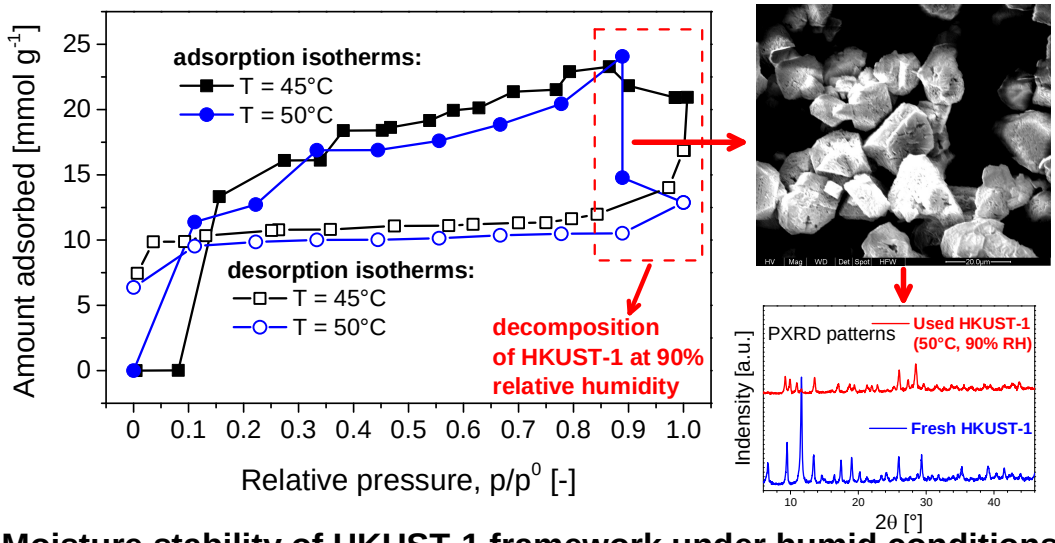

Moisture stability of HKUST-1 framework under humid conditions

1. Introduction

Flue gases from power plants and industrial furnaces are major sources of CO_2 emissions to the atmosphere. Emitted at 50–75ºC and 0–1 barG [1], flue gases contain large amounts of CO_2, as much as 5–15 vol.%, together with other gases such as nitrogen (70–75 vol.%) and water vapour (5–7 vol.%), depending on the fuel being used [1, 2]. Novel combustion technologies, such as oxyfuel combustion can provide flue gas streams with over 99 vol.% CO_2 concentration, facilitating the CO_2 capture [3]. However, the target concentration of CO_2 in the exhaust clean gas to be released into the atmosphere is only 0.03 vol.% [4].

Post combustion capture of CO_2 based on adsorbent capture technologies, especially on porous solid adsorbents, *e.g.* pressure swing adsorption [5], has received much attention because, in comparison with carbonates or alkanolamines solvents, solid adsorbents are easier to handle [1] and more economical for regeneration (in terms of energy consumption) [1, 6]. In general, for potential practical applications, a solid adsorbent with a CO_2 adsorption capacity of *ca.* 4 mmol g^{-1} is considered to be economically viable for CO_2 capture [5]. However, operational costs could be further reduced if increases in adsorbent working capacity are coupled with increases in the CO_2/N_2 selectivity [5] and thermal and moisture stability.

Various porous adsorbents have been investigated for CO_2 adsorption, including activated carbons, zeolites and metal-organic frameworks (MOFs) [2, 7, 8]. Amongst these, MOFs have been recently recognised as promising alternatives for selective gas adsorption due to

their ease of manipulation in porous structures and chemical properties [9, 10], hence altering their adsorption capacity, selectivity and stability (thermal and moisture) properties.

Cu-BTC framework, *i.e.* Copper benzene-1,3,5-tricarboxylate or HKUST-1 [11], is one of the most extensively studied MOFs for gas separation [12-15] and storage [16, 17] due to its high surface area (normally in a range of 600–1600 m^2 g^{-1} for samples synthesised in a laboratory), large pore volume (*ca.* 0.70 cm^3 g^{-1}) [18] and good thermal stability (thermally stable up to 350ºC) [19]. HKUST-1 has been successfully prepared using various synthetic methods, including conventional hydrothermal/solvothermal methods [11, 18-21] and alternative synthetic methods based on unconventional energy sources (*i.e.* microwave [18, 22] and ultrasound [18, 23]), mechanochemical [18, 24] and electrochemical methods [25]. Although alternative synthetic methods offer quantitative yields of HKUST-1 at the laboratory scale with relatively short reaction times, they usually result in products of inconsistent yields, porous structures and crystallinity. For example, a microwave-assisted solvothermal synthesis has been developed as the fastest method to produce pure HKUST-1 (30 min synthesis time [18]). However, the yields and qualities of the resulting product and the optimum reaction conditions are found to significantly depend on the choice of the microwave system [18, 22]. Considering the possible hot spot formation in the system using alternative energy for intensive heating, the scalability of such processes to produce consistent high-quality materials is limited. Therefore, the conventional synthetic methods are more attractive for large-scale manufacture of HKUST-1, though the balance between reactions conditions (temperature and synthesis time) and by-product (*e.g.* Cu_2O) formation is still a challenge.

To date, the primary research interest of CO_2 adsorption on HKUST-1 has been focused on the manipulation of the CO_2 adsorption capacity/selectivity by using materials design strategies [17, 26] or postsynthetic modification approaches [15]. However, apart from tuning the CO_2/N_2 selectivity to increase the CO_2 capture efficiency, the effect of the presence of water vapour in flue gas streams also needs to be considered to properly assess their performance as potential CO_2 capture materials. Sensitivity to water vapour is widely considered to be a major weakness of MOFs as adsorption materials that could destroy their potential advantages from an application perspective [27]. HKUST-1 is hydrophilic and both theoretical [28-30] and experimental [31] investigations have shown the strong affinity of water molecules to copper centres in the HKUST-1 framework. Therefore, understanding the

moisture stability of MOFs under the appropriate conditions for the CO_2 capture from flue gases (50–75ºC and 0–1 barG) is necessary.

So far, only a few theoretical [28] and experimental investigations [32-34] on the stability of HKUST-1 have been reported. BET surface area of HKUST-1 was found to decrease by 52% (from 1340 to 647 m^2 g^{-1}) after an extreme water stability test, *i.e.* 24 h immersion in deionised water at 50ºC [32]. An investigation based on ^1H and ^{13}C NMR spectroscopy also revealed that water adsorption (at room temperature) has a strong influence on the carboxylate carbon resonance, jeopardising the Cu-BTC coordination [33]. Rezk et al. evaluated several MOFs for adsorption cooling and demonstrated the thermal instability of HKUST-1 based on the clear hysteresis between the measured adsorption and desorption isotherms at 52ºC [34]. Despite these preliminary studies, there is no systematic evaluation of MOF's stability in the region of interest for flue gases CO_2 capture, especially when it comes to obtaining the critical parameters that contribute to the evaluation of moisture sensitivity of MOFs under humid conditions.

In this work, we use the HKUST-1 framework as the model MOF, presenting (*i*) an improved synthesis of HKUST-1 using static hydrothermal methods to enable its large-scale production and (*ii*) the experimental investigation of gas adsorption on HKUST-1 under conditions close to real flue gas streams with special focus on its performance under humid conditions (up to 90% relative humidity). The understanding of the moisture stability of HKUST-1 framework will (*i*) provide a holistic overview of the stability study of HKUST-1 framework under the dynamic vapour adsorption conditions and (*ii*) be a guide to future improvements in the design and modification of this highly-promising material in flue gas treatment applications.

2. Experimental

Materials

Copper (II) nitrate trihydrate [$Cu(NO_3)_2{\cdot}3H_2O$, 99%] and benzene-1,3,5 tricarboxylic acid (BTC, 95%) were obtained from Sigma Aldrich and ethanol (absolute, EtOH) was purchased from Fisher. All materials were used as received without further purification.

Hydrothermal synthesis of HKUST-1framework

The general procedure of preparing HKUST-1framework using hydrothermal synthesis was based on the method reported by Schlichte et al. [20] where BTC (0.42 g, 2 mmol) was dissolved in 24 ml of 50:50 vol.% mixture of ethanol and deionised water. The mixture was stirred for 10 min until a clear solution was obtained. Then $Cu(NO_3)_2{\cdot}3H_2O$ (0.875 g, 3.62 mmol) was added to the mixture and stirred thoroughly for another 10 min. Once the reactants were completely dissolved in the solvent, the resulting blue solution was transferred to a 50 ml Teflon-lined stainless steel autoclave and heated to 100ºC for the crystallisation to occur. After synthesis, the reactor was cooled to room temperature and a blue crystalline powder was formed. The powder was then filtered and washed thoroughly with a 60 ml mixture of water and ethanol (% v/v of water = 50%). The product was finally activated under vacuum at 120ºC for 16 h and stored in closed vials in an oven at 60ºC for further experiments.

Characterisation of HKUST-1 framework

Powder X-ray diffraction (PXRD) was carried out on a Rigaku Miniflex diffractometer (Cu$K\alpha$ radiation, 30 kV, 15 mA, λ = 1.5406 Å) using a step scan mode (0.03º per step) with a range of $5º < 2\theta < 46º$. Scanning electron microscopy (SEM) analyses were carried out using a FEI Quanta 200 ESEM equipment with a high voltage mode of 20 kV. Gold coating of samples was performed using an Emitech K550X sputter coater under vacuum conditions of 1×10^{-4} mbar. Nitrogen adsorption/desorption isotherms at −196ºC were obtained using a Micrometrics ASAP 2020 analyser. Surface area was determined using the Brunauer-Emmett-Teller (BET) method. The degassing was carried out at 180ºC overnight under vacuum prior to the measurement. Thermogravimetric analyses (TGA) were carried out with a TA Q5000 (V3.15 Build 263) thermogravimetric analyser. The temperature range was 0–450ºC with a heating rate of 5ºC min^{-1} in a nitrogen atmosphere (25 mL min^{-1}). Differential Scanning Calorimetric (DSC) analysis was carried out using a Mettler DSC30 instrument, with explorer software to perform the peak analysis. The DSC instrument was calibrated with indium prior to analysis (accuracy of the enthalpy measurements = ±1%). Samples were heated and cooled at a rate of 5ºC min^{-1} and the scan was completed over a range of 50 to 350ºC.

Single-component adsorption equilibrium of CO_2, N_2 and water vapour on HKUST-1 framework

CO_2 and N_2 adsorption/desorption experiments were carried out using an intelligent gravimetric analyser (Hiden IGA-001). Samples were first treated thermally at 100ºC for 3 h before being heated up to 200ºC (2 ºC min^{-1}) and kept at 200ºC for 8 h under vacuum. Before the measurement, helium adsorption at 20ºC was measured to assess the buoyancy effect and determine the density of the samples. The measured density was then used for CO_2 and N_2 adsorption/desorption isotherms acquisition at 20ºC and 60ºC from vacuum to 20 barG.

Water vapour adsorption isotherms were measured gravimetrically using a dynamic vapour adsorption analyser (Surface Measurements Systems, DVS 1). The analyser was housed inside an environmental chamber at a constant temperature to ensure a stable baseline and the accurate delivery of required relative humidity. Relative humidity is controlled by mixing dry nitrogen and saturated water vapour in appropriate proportions using mass flow controllers. Prior to the sample loading, dry nitrogen at 2 barG pressure was used to purge the head of the balance (Cahn D200) to prevent vapour condensation in the balance's head and ensure an accurate measurement. All samples were dried at 0% relative humidity (RH) for 6 h before the measurement of adsorption/desorption isotherms at various vapour partial pressures. The water vapour adsorption isotherms of HKUST-1 were measured at temperatures of 25, 35, 40, 45 and 50ºC with relative humidity values ranging from 0 to 90%.

3. Results and discussion

Improved hydrothermal synthesis of HKUST-1framework

HKUST-1 framework was synthesised following an optimised hydrothermal method based on the original recipe developed by Chui et al. [11], starting from $Cu(NO_3)_2$ salt and H_2O and EtOH mixtures as the reaction media. The original work was carried out at 180ºC for 12 h and obtained a yield of *ca.* 60% [11] due to the formation of Cu_2O as the by-product at 180ºC [11, 21].

Over the past decade, great effort has been made by varying the synthesis temperature and time to improve the quality and yield of HKUST-1 during its hydrothermal synthesis, as summarised in Table 1. In general, it was found that low synthesis temperatures tend to supress the formation of Cu_2O promoting the formation of HKUST-1 with high purity [21]. However, long reaction times are usually required to achieve high yields. Well-shaped pure octahedral crystals of HKUST-1 (evidenced by the SEM analysis) were obtained at 75ºC with a maximum yield of 80% after a prolonged reaction time of 320 h [21]. Most of the previous studies focused on the comparison of the resulting products in terms of BET surface area and pore volume for potential gas adsorption and storage applications. However, only a few studies have investigated the effect of the variation of the synthesis conditions on the yield of HKUST-1 [18, 21]. In order to gain a fundamental understanding on the effect of the synthesis conditions of HKUST-1, a systematic study was carried out.

The yield of HKUST-1 at 100ºC (calculated using Eq. 1, the theoretical yield based on the limiting reactant) increased with the reaction time until it reaches a maximum value of 89.4% at 24 h (**Fig. 1**). Further increase of the reaction time beyond this time results in a decrease of the yield, in agreement with the observations by Seo et al [22]. Prolonged contact time between the formed crystals and the synthesis medium can lead to the re-dissolution of HKUST-1 due to the shift of equilibrium between the crystallised and dissolved material. In addition, the as-made sample obtained at 100ºC (before activation under vacuum) has a blue colour, while the colour of the activated framework is dark violet (**Fig. 1**). The colour change of HKUST-1 framework before and after activation is caused by the removal of covalently bounded water molecules from copper centres [20] and the associated *d-d* transition of copper ions [16].

$$\text{Yield of HKUST-1 \%} = \frac{\text{mass of as-made HKUST-1}}{\text{theoretical mass based on the limiting reactant}} \times 100\% \qquad (1)$$

Table 1
Summary of reaction conditions and yields for the hydrothermal synthesis of HKUST-1 frameworks.

Year	*T* [°C]	*t* [h]	Solvents	Yield [%]	BET surface area [$m^2\ g^{-1}$]	Ref.
1999	180	12	H_2O + EtOH	*ca.* 60	692.2	[11]
2002	110	18	H_2O + EtOH	*ca.* 74*	964.5	[12]
2004	120	12	H_2O + EtOH	*ca.* 60	N/A	[20]
2006	110	15	H_2O + EtOH	N/A	N/A	[35]
2007	85	8	H_2O + EtOH + DMF EtOH + DMF + CH_2Cl_2	N/A N/A	1482 698	[36]

2008	120	14	H_2O + EtOH	N/A	1510	[37]
			EtOH	N/A	1253	
2008	95	15	H_2O + EtOH	N/A	N/A	[38]
2009	75	320	H_2O + EtOH	*ca.* 80	N/A	[21]
2010	120	24	H_2O + EtOH	*ca.* 94*	1143	[18]
			DMF	N/A	1323	
2012	110	18	H_2O + EtOH	N/A	1055	[16]

* HKUST-1 yield was calculated based on substrate - $Cu(NO_3)_2$.

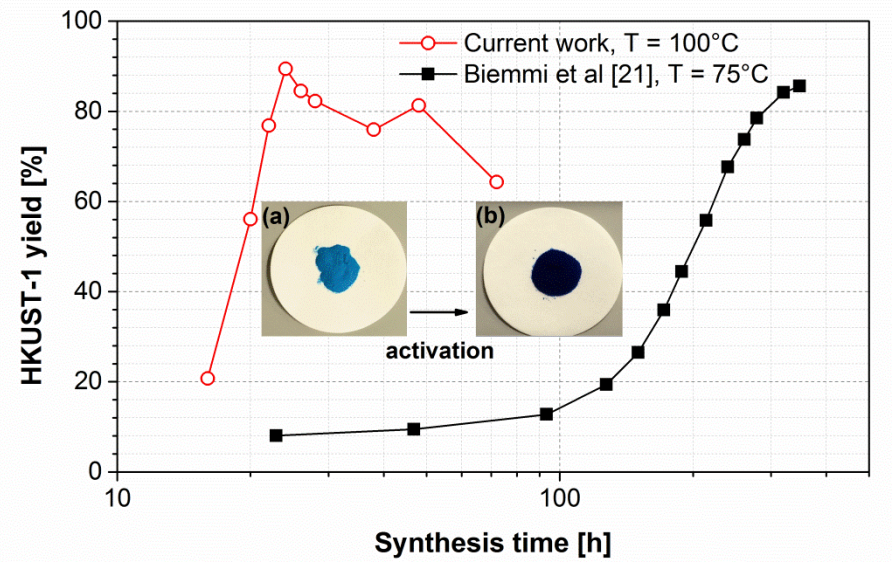

Fig. 1. Optimised yields of HKUST-1 at different synthesis temperatures as a function of reaction time in comparison to previous work in the literature [21]. Inset: HKUST-1 framework synthesised at 100°C under static hydrothermal conditions. Inset: HKUST-1 samples (a) as made sample and (b) activated sample.

Characterisation of HKUST-1frameworks

The crystallinity of the synthesised samples as a function of reaction time at 100°C was investigated using PXRD as shown in **Fig. 2**. HKUST-1 is one of the most frequently investigated MOFs and its crystalline phase is usually exemplified by a PXRD pattern with characteristic peaks at $2\theta \approx 6.5^o$, 9.5^o, 11.5^o and 13.4^o [11, 16, 20-22], in agreement with our work, confirming the formation of HKUST-1 crystalline phase. The variations in intensities of the different diffraction peaks can be attributed to the degree of hydration of different samples since HKUST-1 crystals can rapidly absorb moisture from the air [16, 20]. The characteristic diffraction peaks of Cu_2O at $2\theta \approx 36.4^o$, 42.3^o and 43.3^o [21] are not observed in the PXRD patterns of samples synthesised at 100°C under static hydrothermal conditions suggesting high purity of the HKUST-1 product.

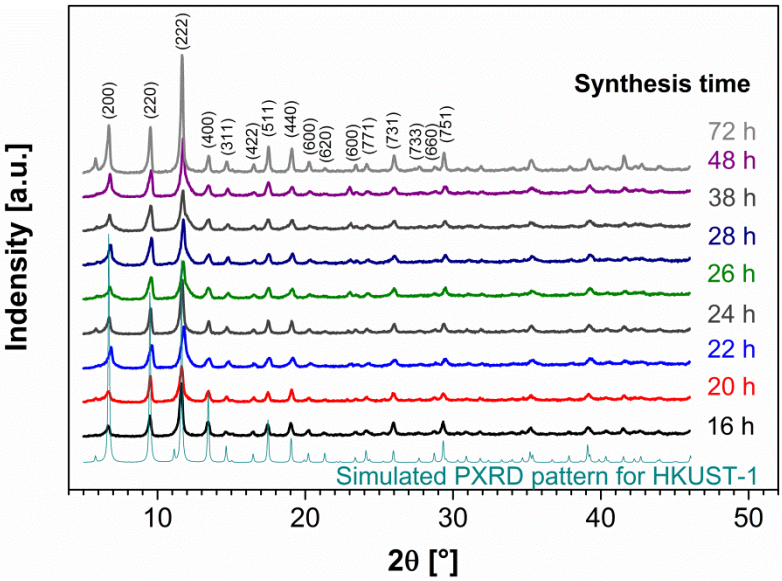

Fig. 2. PXRD patterns of HKUST-1 frameworks synthesised at different reaction times under static hydrothermal conditions at 100ºC.

The effect of the synthesis time on the morphology of HKUST-1 crystals at 100ºC was studied using SEM characterisation. Representative pictures are shown in **Fig. 3**. For samples synthesised with reaction time < 24 h, clean crystals with average sizes of *ca.* 20 µm were obtained (**Fig. 3a and 3b**). These crystals are well-defined octahedrons with sharp edges [16, 21, 39].

The octahedral morphology of HKUST-1 crystals phase becomes less defined for a reaction time of 28 h, *i.e.* losing the sharp edges while maintaining the crystal size at *ca.* 20 µm, as seen in **Fig. 3c**. Further increase of the reaction time to 38 h and above led to the deformation of crystals with a shrinking of crystal sizes and losing the octahedral shapes completely (**Fig. 3d**). The change of HKUST-1 morphology as the synthesis time increases is directly related to the decrease in yield, indicating the re-dissolution of HKUST-1 crystals in the reaction media caused by the prolonged reaction time. Similar observations have been reported in the hydrothermal synthesis of ceramic materials [40, 41].

In addition, **Fig. 3d** also reveals that prolonged synthesis time results in the formation of small particles/crystals on the surface of octahedrons. These small particles are possibly the re-crystallised HKUST-1 phase or other by-products formed at long reaction time at 100ºC. Further investigation is needed to understand the equilibrium dynamics between the crystallised MOFs and the MOFs that remain in the solution for optimising the synthesis of MOFs under hydrothermal conditions.

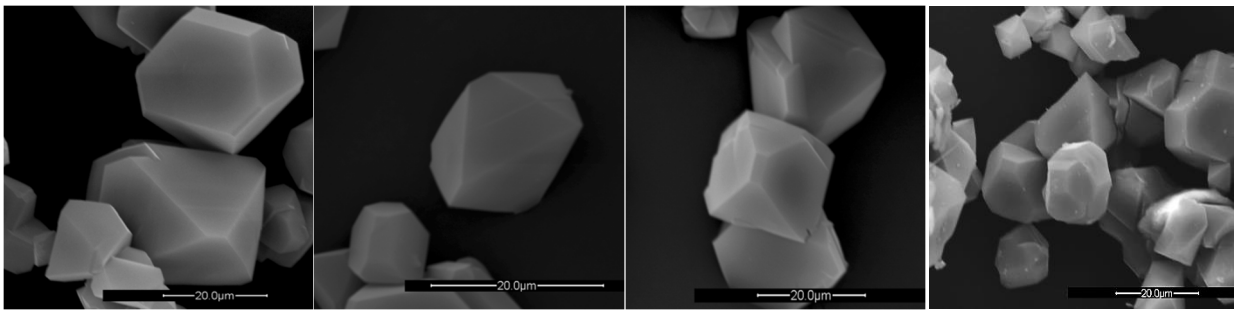

Fig. 3. Influence of the synthesis time on the morphology of HKUST-1 frameworks for the hydrothermal synthesis at 100ºC. SEM images of synthesised HKUST-1 samples at reaction times of (a) 16 h, (b) 22 h, (c) 28 h and (d) 38 h.

Nitrogen adsorption and desorption isotherms were measured on a sample that was synthesised at 100ºC and 24 h. The BET specific surface areas and pore volumes were calculated as 1507 m^2 g^{-1} and 0.609 cm^3 g^{-1}, respectively, comparable to the previously reported values (Table 1 and refs [14, 42]). Variations in measured BET surface areas and pore volume from different investigations may be attributed to the difference in post-synthesis work-up procedures, *i.e.* washing and activation of the HKUST-1 samples.

TGA (**Fig. 4**) shows the thermal stability of the HKUST-1 framework synthesised in this work at 100ºC for 24 h. Dehydration of the material takes place up to *ca.* 180ºC with total weight loss of *ca.* 20 wt.%, corresponding to three water molecules per copper centre in the framework (Fully hydrated HKUST-1 is reported to hold up to 40 wt.% water [12]). DSC result correlates well to the TGA showing that an endothermic peak (100–280ºC) due to the dehydration of HKUST-1. HKUST-1 was found to be thermally stable up to 280ºC before starting to gradually disintegrate at higher temperatures [12, 22]. The weight loss of decomposition was measured as 36%, which is very close to the theoretical loss of 36.7% accounting for decomposition into Cu_2O and CuO [22] (PXRD analysis of the residue after TGA is shown in the inset of **Fig. 4**). Two exothermic peaks were discovered by DCS analysis after 280ºC with first exothermic peak (280–300ºC) corresponds to the formation of Cu_2O [43] and the second one corresponds to the phase transformation of Cu_2O to CuO [44].

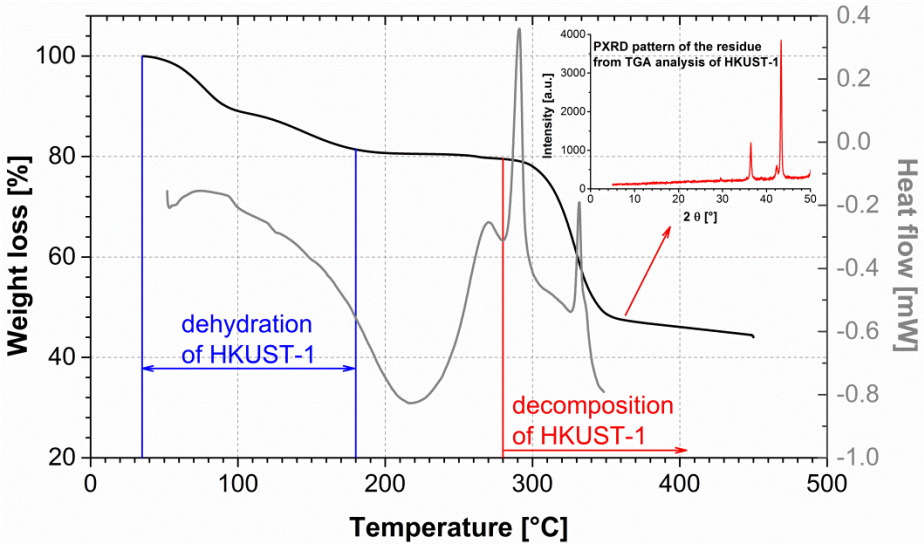

Fig. 4. TGA (under nitrogen) and DSC analysis of HKUST-1 framework synthesised at 100ºC and 24 hours under static hydrothermal conditions. Inset: PXRD pattern of the residual material after TGA.

CO_2 and N_2 adsorption on to HKUST-1framework

The experimental adsorption isotherms of CO_2 and N_2 on to HKUST-1 were measured over a pressure range of 0–20 barG at 20 and 60ºC, respectively, as shown in **Fig. 5a**. No hysteresis loops were detected between the adsorption and the desorption isotherms suggesting no tensile strength effect caused by ink-bottle type pores. The adsorption capacity on HKUST-1 decreases with the increase in temperature for both gases. HKUST-1 has a higher affinity to CO_2 than to N_2, evidenced by the significant difference in adsorption capacities at any pressure. **Fig. 5a** also presents the correlation of the CO_2 and N_2 isotherms with the Langmuir model, with a squared residual (R^2) larger than 0.9995.

Considering the application of HKUST-1 as potential materials for CO_2 adsorption from flue gases, only the data from the pressure range of (0–1 barG) at 60ºC is of interest. The average ratio of adsorption uptake of CO_2 to N_2 under such conditions (60ºC and 0–1 barG) is found as *ca.* 7.6. The isotherms for both gases can be considered linear at these conditions, therefore, an estimate in the selectivity of the adsorbent can be obtained from the ratio of the affinity coefficients in the Langmuir model, which is *ca.* 47%.

Obtained constants of the Langmuir model were also used to calculate the isosteric heat of adsorption for CO_2 and N_2 adsorption as shown in **Fig. 5b** [14, 45]. The calculated isosteric heat of CO_2 and N_2 adsorption is found to be almost constant over the range of adsorbate

loading, indicating an energetically homogenous surface of the adsorbent (HKUST-1), *i.e.* all the available adsorption sites have the same adsorption energy for the probing gases [46, 47]. The obtained values of isosteric heat for CO_2 and N_2 adsorption onto HKUST-1 framework are *ca.* 27 kJ mol^{-1} and *ca.* 14.5 kJ mol^{-1}, respectively, which are in typical range for physisorption.

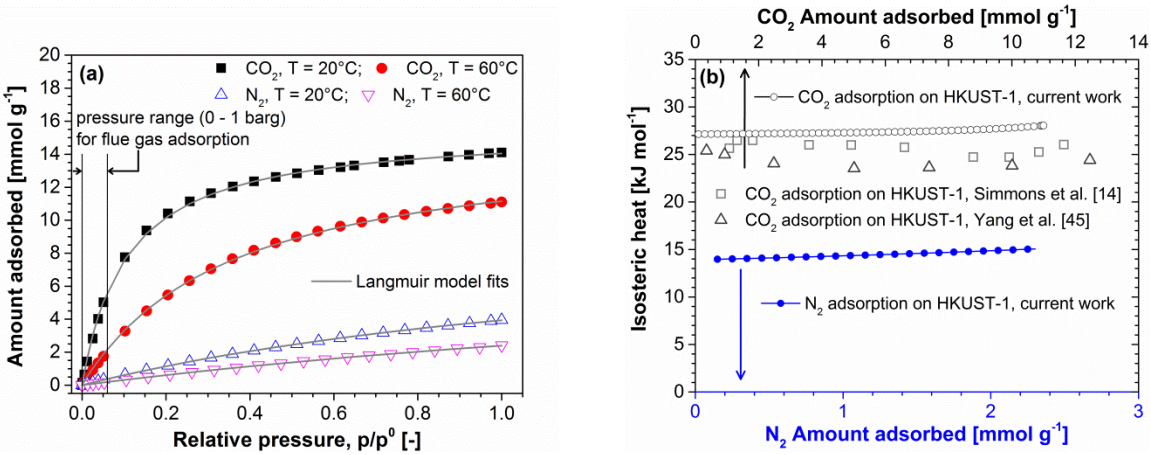

Fig. 5. (a) Single-component CO_2 and N_2 adsorption isotherms for HKUST-1 at 20 and 60ºC over a pressure range of 0–20 barG. (b) Calculated isosteric heat of adsorption as a function of CO_2 and N_2 uptake onto HKUST-1.

Dynamic water vapour adsorption onto HKUST-1 framework

Fig. 6a shows the water vapour dynamic uptake of HKUST-1 framework at 25ºC. It was found that the interaction between the adsorbed water molecules and HKUST-1 is strong, *i.e.* significantly longer time was required for desorption to reach equilibrium than that of adsorption at the same vapour partial pressure (**Fig. 6a**). The water adsorption isotherm on HKUST-1 is shown in **Fig. 6b**. The relative pressure is defined as the ratio of the water vapour pressure to the measured saturation pressure at a given temperature. The results obtained are consistent with data reported in the literature [27].

The water adsorption isotherm at 25ºC shows two steep slopes and one intermediate flat region, characteristic of a type II adsorbent. The first rising slope at a low relative vapour pressure range (0–0.2) is largely attributed to the preferential adsorption of water vapour in the region near the copper atoms of the primary pores, *i.e.* Cu-BTC cages. Molecular simulations have shown that water molecules have a strong affinity to the copper centres due to their large dipolar moment [28]. Therefore, the interaction between the water vapour and

unsaturated copper centres is expected as immediate under humid conditions, leading to a sharp increase of water uptake at the initial stage of adsorption.

The shallow slope over the relative pressure range between 0.2 and 0.8 corresponds to the filling of the Cu-BTC cages caused by the formation of water clusters due to hydrogen bonding [48], *i.e.* saturation of the primary pores. This hypothesis was based on the theoretical calculation of Henry coefficients using the grand-canonical Monte Carlo simulations [28]. Simulation results show that the Henry coefficient of water molecule adsorption within the void space of Cu-BTC cages (*ca.* 4.6×10^{-6} mol kg^{-1} Pa^{-1}) is significantly lower than one for the unsaturated copper centres (*ca.* 2.0×10^{-2} mol kg^{-1} Pa^{-1}) [28].

The final rise of adsorbed uptake of water vapour, which occurs at high relative pressure of > 0.8, is associated with the adsorption of water molecules in the micropores of the side pockets and in the outer surface of the crystal. The nature of these side pockets in the HKUST-1 framework is believed to be hydrophobic [49], *i.e.* the reluctance to form strong interaction with water molecules, and hence the filling of the side pockets with water vapour only occurs at the final stage of adsorption with relatively high vapour partial pressure. The adsorption isotherms at 35 and 50ºC are similar to the one at 25ºC with shifted relative pressure ranges for relevant adsorption stages.

HKUST-1 frameworks have shown clear hysteresis between adsorption and desorption isotherms at 25ºC but in a thermodynamically impossible manner, *i.e.* the crossing of desorption isotherm with the adsorption isotherm. Such hysteresis phenomena are likely caused by the partial decomposition during the adsorption step. Therefore, in the desorption step, a significant amount of water desorbs from the decomposed HKUST-1 due to the weak binding between water molecules and the decomposed solid phase resulting in a steep decline of the desorption isotherm. Furthermore, it is also found that not all the water was desorbed when the partial pressure of water was returned to zero, indicating the retention of water molecules within the partially decomposed framework. This phenomenon is probably the result of the water-unsaturated copper centres strong binding. The theoretical value of adsorbed water on unsaturated copper sites can be estimated as 5 mmol g^{-1} assuming x molecules of water per copper atom, which is close to the remaining uptake (*i.e.* 6.73 mmol g^{-1}) at the end of desorption process. Such absorbed water molecules on unsaturated copper sites can only be removed by activation at high temperatures.

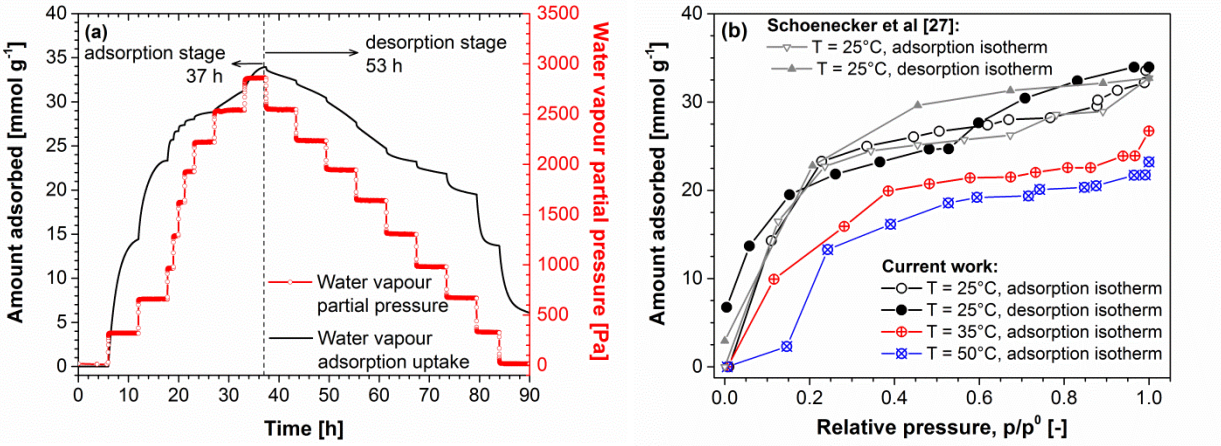

Fig. 6. (a) Temporal water vapour adsorption and desorption at different vapour partial pressures for HKUST-1 framework at 25ºC and 90% relative humidity. (b) Water adsorption and desorption isotherms on HKUST-1 at 25ºC (up to 90% RH, in comparison to literature data [27]), 35ºC (up to 90% RH) and 50ºC (up to 70% RH).

The water vapour adsorption capacity of HKUST-1 framework at 25ºC and ambient pressure (2850 Pa vapour partial pressure) was measured as 33.3 mmol g^{-1} [27, 49, 50], as seen in **Fig. 6b.** Vapour adsorption capacity was found to decline with increasing the temperature (**Fig. 6b**). The measured adsorption uptake dropped by *ca.* 35% with increasing adsorption temperature from 25ºC to 50ºC. Considering conditions of the flue gas emission (50–60ºC and atmospheric pressure), it is apparent that the water vapour adsorption is much more preferable than CO_2 adsorption, *i.e.* considerable higher water vapour uptake of *ca.* 21.7 mmol g^{-1} at 50ºC (up to 70% RH) in comparison with the CO_2 uptake of *ca.* 1.75 mmol g^{-1} under similar conditions. This is further evidenced by comparing the isosteric heat of water vapour adsorption with CO_2 adsorption (*vide supra*, **Fig. 5b**). The isosteric heat of water vapour adsorption was estimated (using the Dual Sites Langmuir Freundlich model [51]) as 48.6 kJ mol^{-1}, and comparable with the reported values, *i.e.* 48.5 and 50.7 kJ mol^{-1} [34, 52], suggesting the possible chemisorption of water vapour on HKUST-1. This is can be explained by (*i*) the strong interaction between the unsaturated copper centres and water molecules and (*ii*) the hydrophilic nature of HKUST-1 with water contact angles close to 0° [53].

Moisture stability of HKUST-1 framework

The PXRD patterns of fresh (after activation) and used HKUST-1 (after water vapour adsorption) are shown in **Fig. 7**. For the sample used in the dynamic vapour adsorption experiment at 25ºC, the characteristic peaks of HKUST-1 framework at $2\theta \approx 6.5º$, 9.5º, 11.5º

and 13.4º are still identifiable, indicating that the crystal structure of HKUST-1 was primarily maintained after holding a large amount of water (33.3 mmol g^{-1}) at relative humidities up to 90%. However, PXRD patterns also revealed a slight increase of the amorphous background in comparison with the fresh, consistent with a partial degradation of the material. At the highest temperature studied, *i.e.* 50ºC, the HKUST-1 framework structure remains up to 70% RH but collapses at 90% RH, as evidenced by the PXRD analysis (**Fig. 7**).

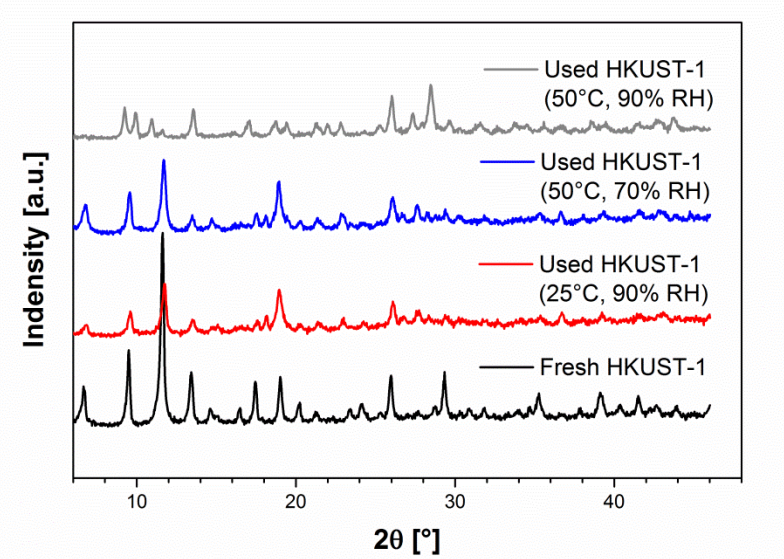

Fig.7. PXRD patterns for used HKUST-1 from dynamic water vapour adsorption under various conditions in comparison to the PXRD pattern of fresh HKUST-1.

The framework structure of HKUST-1 was found to irreversibly change by increasing the water vapour partial pressure at high temperatures (40–50ºC). Sudden drops in vapour uptake were measured at high relative pressure, as seen in **Fig. 8,** which indicates the collapse of the porous structure of HKUST-1. In comparison with the fresh sample, the PXRD pattern of the material after water adsorption (at 50ºC and 90% RH) had totally lost the characteristic diffraction peaks of the HKUST-1 crystal structure, *i.e.* the diffraction peaks at $2\theta \approx 6.5^{o}$ and 11.5º are no longer noticeable (**Fig. 7**). SEM characterisation (**Fig. 8 inset**) also shows irregular shapes in used samples with visible cracks on the crystal's surface, having lost the HKUST-1's octahedral shape and its sharp edges. A summary of the temperature and relative humidity range for hydrothermally stable HKUST-1 under dynamic vapour adsorption conditions are presented in **Table 2**.

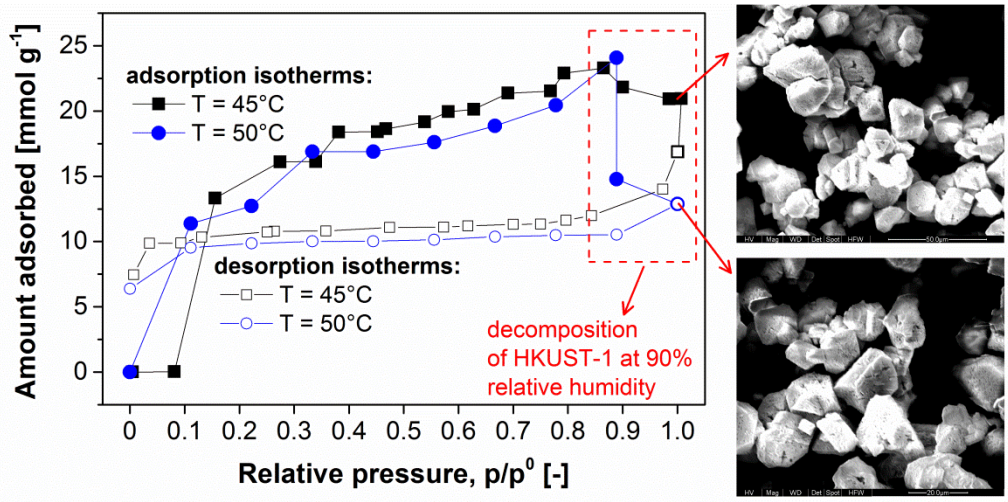

Fig. 8. Water adsorption and desorption isotherms for HKUST-1 framework at 45ºC and 50ºC (up to 90% RH). Inset: SEM images for the used HKUST-1 after water adsorption at 50ºC with 90% RH.

Table 2
Conditions for maintaining moisture stability of HKUST-1 framework and the corresponding maximum water vapour adsorption capacity.

T [ºC]	RH [%]	p_{vapour} [Pa]	Maximum H_2O adsorption uptake [mmol g^{-1}]
25	0–90	0–2850	33.3
35	0–90	0–4250	27.0
40	0–80	0−6000	25.0
45	0–70	0–8200	23.0
50	0–70	0–8990	21.6

The strong bonds between water molecules and the unsaturated metal sites in the HKUST-1 framework are believed to induce the decomposition of the material at high adsorption temperatures and high relative humidity. Under such conditions, the aggregation of adsorbed water molecules near the metal sites may gradually displace the coordinated carboxylate groups of BTC ligands from the copper centres leading to the final break of the metal-ligand coordination. Such a phenomenon was previously observed in the MOF-5 framework [$Zn_4O(BDC)_3$] (DBC – Benzene-1,4-dicarboxylic acid) upon its exposure to humid air, in which the humid air not only displaced the ligand coordination of MOF-5 from the zinc metal centres, but also penetrated into the metal building blocks and changed the structure into MOF-69C [$Zn_3(OH)_2(BDC)_2$], which is hydrothermally unstable [9, 54]. Here we have shown that the crystal morphology and the microstructure of HKUST-1 changes upon exposure to water at high temperatures. The same degradations were also recently reported at room temperature after one year exposure to the atmosphere takes place over longer periods of time. The same structure's degradation has been observed recently when HKUST-1 was naturally stored at room temperature for a year [55]. A re-crystallisation method (using

synthesis media, ethanol or ethanol/water mixture) was also proposed for the reconstruction of HKUST-1.

4. Conclusions

This paper presented a further refinement on the hydrothermal synthesis of HKUST-1. Here we obtained an optimised procedure that maximises the yield of HKUST-1 (up to 89.4% at 100ºC) while maintaining a high quality product, by systematically varying the reaction temperature and reaction time. This synthetic study provides a good understanding of the effect of the synthetic hydrothermal parameters of HKUST-1 for the design of a potential manufacturing process.

Prepared HKUST-1 samples were fully characterised and single-component adsorption experiments were conducted to evaluate HKUST-1's performance under relevant flue gas adsorption conditions (45–60ºC, 0–1 barG). The preference of gas adsorption onto HKUST-1 under such conditions is water vapour (*ca.* 21.7 mmol g^{-1}) > CO_2 (*ca.* 1.75 mmol g^{-1}) > N_2 (*ca.* 0.17 mmol g^{-1}). Dynamic water vapour adsorption measurements were used to assess the moisture stability of HKUST-1. An envelope of conditions (temperature, relative humidity and vapour partial pressure) was experimentally established for maintaining the porous structure of HKUST-1 framework under humid conditions. Irreversible decomposition of HKUST-1 framework was noticed in dynamic vapour adsorption experiments caused by the partial displacement of organic linkers from the copper centres by aggregated water molecules, leading to the deterioration in the adsorption capacity of HKUST-1.

Acknowledgements

This work was supported by the School of Chemical Engineering and Analytical Science, The University of Manchester (pump priming project: P118086) and the EPSRC (EP/L020432/1). NAJ is grateful to the Higher Committee for Education Development in Iraq for her postgraduate research scholarship. We thank Prof. R. Davey for the PXRD measurements.

References

[1] R. Sabouni, H. Kazemian, S. Rohani, Carbon dioxide capturing technologies: A review focusing on metal organic framework materials (MOFs), Environ. Sci. Pollut. Res. 21 (2014) 5427−5449.
[2] A.-H. Lu, G.-P. Hao, Porous Materials for Carbon Dioxide Capture, Springer-Verlag Berlin Heidelberg, 2014.
[3] L.T. Murciano, V. White, F. Petrocelli, D. Chadwick, Sour compression process for the removal of SOx and NOx from oxyfuel-derived CO_2, Energy Procedia 4 (2011) 908−916.
[4] U. Jecht, 2004, Flue Gas Analysis in Industry, second ed., USA, TESTO, p.16.
[5] M.T. Ho, G.W. Allinson, D.E. Wiley, Reducing the cost of CO_2 capture from flue gases using pressure swing adsorption, Ind. Eng. Chem. Res. 47 (2008) 4883−4890.
[6] D. Aaron, C. Tsouris, Separation of CO_2 from flue gas: A review, Separ. Sci. Technol. 40 (2005) 321−348.
[7] C. Lu, H. Bai, B. Wu, F. Su, J.F. Hwang, Comparative study of CO_2 capture by carbon nanotubes, activated carbons, and zeolites, Energy Fuels 22 (2008) 3050−3056.
[8] D. Bonenfant, M. Kharoune, P. Niquette, M. Mimeault, R. Hausler, Advances in principal factors influencing carbon dioxide adsorption on zeolites, Sci. Technol. Adv. Mater. 9 (2008) 013007.
[9] J. Liu, P.K. Thallapally, B.P. McGrail, D.R. Brown, J. Liu, Progress in adsorption-based CO_2 capture by metal-organic frameworks, Chem. Soc. Rev. 41 (2012) 2308−2322.
[10] A. Schneemann, V. Bon, I. Schwedler, I. Senkovska, S. Kaskel, R.A. Fischer, Flexible metal-organic frameworks, Chem. Soc. Rev. 43 (2014) 6062−6096.
[11] S.S. Chui, M.F. Lo, J.P. Charmant, A.G. Opren, I.D. Williams, A chemically functionalizable nanoporous material $[Cu_3(TMA)_2(H2O)_3]_n$, Science 283 (1999) 1148−1150.
[12] Q. Min Wang, D. Shen, M. Bülow, M. Ling Lau, S. Deng, F.R. Fitch, N.O. Lemcoff, J. Semanscin, Metallo-organic molecular sieve for gas separation and purification, Microporous and Mesoporous Mater. 55 (2002) 217−230.
[13] J. Liu, J.T. Culp, S. Natesakhawat, B.C. Bockrath, B. Zande, S.G. Sankar, G. Garberoglio, J.K. Johnson, Experimental and theoretical studies of gas adsorption in $Cu_3(BTC)_2$: An effective activation procedure, J. Phys. Chem. C 111 (2007) 9305−9313.
[14] J.M. Simmons, H. Wu, W. Zhou, T. Yildirim, Carbon capture in metal-organic frameworks − A comparative study, Energy Environ. Sci. 4 (2011) 2177−2185.
[15] X. Yan, S. Komarneni, Z. Zhang, Z. Yan, Extremely enhanced CO_2 uptake by HKUST-1 metal-organic framework *via* a simple chemical treatment, Microporous and Mesoporous Mater. 183 (2014) 69−73.
[16] K.-S. Lin, A.K. Adhikari, C.-N. Ku, C.-L. Chiang, H. Kuo, Synthesis and characterization of porous HKUST-1 metal organic frameworks for hydrogen storage, Int. J. Hydrogen Energy 37 (2012) 13865−13871.
[17] K. Peikert, F. Hoffmann, M. Froba, Amino substituted $Cu_3(btc)_2$: a new metal-organic framework with a versatile functionality, Chem. Comm. 48 (2012) 11196−11198.
[18] M. Schlesinger, S. Schulze, M. Hietschold, M. Mehring, Evaluation of synthetic methods for microporous metal-organic frameworks exemplified by the competitive formation of $[Cu_2(btc)_3(H_2O)_3]$ and $[Cu_2(btc)(OH)(H_2O)]$, Microporous and Mesoporous Mater. 132 (2010) 121−127.
[19] Y.-R. Lee, W.-S. Ahn, J. Kim, Synthesis of metal-organic frameworks: A mini review, Korean J. Chem. Eng. 30 (2013) 1667−1680.
[20] K. Schlichte, T. Kratzke, S. Kaskel, Improved synthesis, thermal stability and catalytic properties of the metal-organic framework compound $Cu_3(BTC)_2$, Microporous and Mesoporous Mater. 73 (2004) 81−88.
[21] E. Biemmi, S. Christian, N. Stock, T. Bein, High-throughput screening of synthesis parameters in the formation of the metal-organic frameworks MOF-5 and HKUST-1, Microporous and Mesoporous Mater.117 (2009) 111−117.
[22] Y. Seo, G. Hundal, I. Jang, Y. Hwang, C. Jun, J. Chang, Microwave synthesis of hybrid inorganic-organic materials including porous $Cu_3(BTC)_2$ from Cu(II)-trimesate mixture, Microporous and Mesoporous Mater. 119 (2009) 331−337.
[23] Z.-Q. Li, L.-G. Qiu, T. Xu, Y. Wu, W. Wang, Z.-Y. Wu, X. Jiang, Ultrasonic synthesis of the microporous metal-organic framework $Cu_3(BTC)_2$ at ambient temperature and pressure: An efficient and environmentally friendly method, Mater. Lett. 63 (2009) 78−80.
[24] H. Yang, S. Orefuwa, A. Goudy, Study of mechanochemical synthesis in the formation of the metal-organic framework $Cu_3(BTC)_2$ for hydrogen storage, Microporous and Mesoporous Mater. 143 (2011) 37−45.
[25] R. Senthil, S. Senthil, M. Anbu, Efficient electrosynthesis of highly active $Cu_3(BTC)_2$-MOF and its catalytic application to chemical reduction, Microporous and Mesoporous Mater. 168 (2013) 57−64.
[26] K. Peikert, F. Hoffmann, M. Fröba, Fluorine magic: one new organofluorine linker leads to three new metal-organic frameworks, CrystEngComm, 17 (2014) 353−360.

[27] P.M. Schoenecker, C.G. Carson, H. Jasuja, C.J.J. Flemming, K.S. Walton, Effect of water adsorption on retention of structure and surface area of metal-organic frameworks, Ind. Eng. Chem. Res. 51 (2012) 6513−6519.
[28] J.M. Castillo, T.J.H. Vlugt, S.I. Calero, Understanding water adsorption in Cu-BTC metal-organic frameworks, J. Phys. Chem. C 112 (2008) 15934−15939.
[29] S. Calero, P. Gomez-Alvarez, Insights into the Aadsorption of water and small alcohols on the open-metal sites of Cu-BTC *via* molecular simulation, J. Phys. Chem. C 119 (2015) 467−472.
[30] J. Jose Gutierrez-Sevillano, S. Calero, R. Krishna, Selective adsorption of water from mixtures with 1-alcohols by exploitation of molecular packing pffects in Cu-BTC, J. Phys. Chem. C 119 (2015) 3658−3666.
[31] F. Gul-E-Noor, B. Jee, A. Poeppl, M. Hartmann, D. Himsl, M. Bertmer, Effects of varying water adsorption on a $Cu_3(BTC)_2$ metal-organic framework (MOF) as studied by ^1H and ^{13}C solid-state NMR spectroscopy, Phys. Chem. Chem. Phys. 13 (2011) 7783−7788.
[32] P. Küsgens, M. Rose, I. Senkovska, H. Fröde, A. Henschel, S. Siegle, S. Kaskel, Characterization of metal-organic frameworks by water adsorption, Microporous and Mesoporous Mater. 120 (2009) 325−330.
[33] F. Gul-E-Noor, D. Michel, H. Krautscheid, J. Haase, M. Bertmer, Time dependent water uptake in $Cu_3(btc)_2$ MOF: Identification of different water adsorption states by ^1H MAS NMR, Microporous and Mesoporous Mater. 180 (2013) 8−13.
[34] A. Rezk, R. Al-Dadah, S. Mahmoud, A. Elsayed, Characterisation of metal organic frameworks for adsorption cooling, Int. J. Heat and Mass Transfer 55 (2012) 7366−7374.
[35] L. Alaerts, E. Seguin, H. Poelman, F. Thibault-Starzyk, P.A. Jacobs, D.E. De Vos, Probing the Lewis acidity and catalytic activity of the metal-organic framework $Cu_3(btc)_2$ (BTC = benzene-1,3,5-tricarboxylate), Chem. Eur. J. 12 (2006) 7353−7363.
[36] J.C. Liu, J.T. Culp, S. Natesakhawat, B.C. Bockrath, B. Zande, S.G. Sankar, G. Garberoglio, J.K. Johnson, Experimental and theoretical studies of gas adsorption in $Cu_3(btc)_2$: An effective activation procedure, J. Phys. Chem. C 111 (2007) 9305−9313.
[37] M. Hartmann, S. Kunz, D. Himsl, O. Tangermann, S. Ernst, A. Wagener, Adsorptive separation of isobutene and isobutane on $Cu_3(btc)_2$, Langmuir 24 (2008) 8634−8642.
[38] Y. Wu, A. Kobayashi, G.J. Halder, V.K. Peterson, K.W. Chapman, N. Lock, P.D. Southon, C.J. Kepert, Negative thermal expansion in the metal-organic framework material $Cu_3(1,3,5\text{-benzenetricarboxylate})_2$, Angew. Chem. Int. Edit. 47 (2008) 8929−8932.
[39] Q.-X. Luo, X.-D. Song, M. Ji, S.-E. Park, C. Hao, Y.-Q. Li, Molecular size- and shape-selective Knoevenagel condensation over microporous $Cu_3(btc)_2$ immobilized amino-functionalized basic ionic liquid catalyst, Appl. Catal., A 478 (2014) 81−90.
[40] L. Torrente-Murciano, A. Gilbank, B. Puertolas, T. Garcia, B. Solsona, D. Chadwick, Shape-dependency activity of nanostructured CeO_2 in the total oxidation of polycyclic aromatic hydrocarbons, Appl. Catal. B 132−133 (2013) 116−122.
[41] T.E. Bell, J.M. Gonzalez-Carballo, R.P. Tooze, L. Torrente-Murciano, Single-step synthesis of nanostructured gamma-alumina with solvent reusability to maximise yield and morphological purity, J. Mater. Chem. A 3 (2015) 6196−6201.
[42] L. Ge, L. Wang, V. Rudolph, Z. Zhu, Hierarchically structured metal-organic framework/vertically-aligned carbon nanotubes hybrids for CO_2 capture, RSC Adv. 3 (2013) 25360−25366.
[43] M. Sánchez, J. Rams, A. Ureña, Oxidation mechanisms of copper and nickel coated carbon fibers, Oxid. Met. 69 (2008) 327−341.
[44] D. Nunes, L. Santos, P. Duarte, A. Pimentel, J.V. Pinto, P. Barquinha, P.A. Carvalho, E. Fortunato, R. Martins, Room temperature synthesis of Cu_2O nanospheres: optical properties and thermal behavior, Microsc. Microanal. 21 (2015) 108−119.
[45] Q. Yang, C. Xue, C. Zhong, J.-F. Chen, Molecular simulation of separation of CO_2 from flue gases in Cu-BTC metal-organic framework, AIChE J. 53 (2007) 2832-2840.
[46] J.A. Schwarz, C.I. Contescu, Surfaces of Nanoparticles and Porous Materials, CRC Press, New York, 1999.
[47] J.J. McKetta, Encyclopedia of Chemical Processing and Design: Volume 6 - Calcination Equipment to Catalysis, CRC Press, New York,1978.
[48] E.A. Müllera, K.E. Gubbins, Molecular simulation study of hydrophilic and hydrophobic behavior of activated carbon surfaces, Carbon 36 (1998) 1433–1438.
[49] Z. Zhao, S. Wang, Y. Yang, X. Li, J. Li, Z. Li, Competitive adsorption and selectivity of benzene and water vapor on the microporous metal organic frameworks (HKUST-1), Chem. Eng. J. 259 (2015) 79−89.
[50] E. Soubeyrand-Lenoir, C. Vagner, J.W. Yoon, P. Bazin, F. Ragon, Y.K. Hwang, C. Serre, J.S. Chang, P.L. Llewellyn, How water fosters a remarkable 5-fold increase in low-pressure CO_2 uptake within mesoporous MIL-100(Fe), J. Am. Chem. Soc. 134 (2012) 10174−10181.
[51] C. Tien, Adsorption Calculations and Modeling, Butterworth-Heinemann, Boston, 1994.

[52] S.K. Henninger, F.P. Schmidt, H.M. Henning, Water adsorption characteristics of novel materials for heat transformation applications, Appl. Therm. Eng. 30 (2010) 1692−1702.
[53] W. Zhang, Y. Hu, J. Ge, H.-L. Jiang, S.-H. Yu, A facile and general coating approach to moisture/water-resistant metal-organic frameworks with intact porosity, J. Am. Chem. Soc. 136 (2014) 16978−16981.
[54] G.K. Kole, J.J. Vittal, Solid-state reactivity and structural transformations involving coordination polymers, Chem. Soc. Rev. 42 (2013) 1755−1775.
[55] X. Sun, H. Li, Y. Li, F. Xu, J. Xiao, Q. Xia, Y. Li, Z. Li, A novel mechanochemical method for reconstructing the moisture-degraded HKUST-1, Chem. Comm. 51 (2015) 10835−10838.